BBA - Molecular and Cell Biology of Lipids 1866 (2021) 158873

Contents lists available at ScienceDirect

BBA - Molecular and Cell Biology of Lipids

journal homepage: www.elsevier.com/locate/bbalip

Isolated Plin5-deficient cardiomyocytes store less lipid droplets than normal, but without increased sensitivity to hypoxia

Yuchuan Li [a,b], May-Kristin Torp [b], Frode Norheim [a], Prabhat Khanal [a,c], Alan R. Kimmel [d], Kåre-Olav Stensløkken [b], Jarle Vaage [b,e,f], Knut Tomas Dalen [a,g,*]

[a] Department of Nutrition, Institute of Basic Medical Sciences, Faculty of Medicine, University of Oslo, Norway
[b] Department of Molecular Medicine, Institute of Basic Medical Sciences, University of Oslo, Norway
[c] Faculty of Biosciences and Aquaculture (FBA), Nord University, Norway
[d] Laboratory of Cellular and Developmental Biology, National Institute of Diabetes and Digestive and Kidney Diseases, The National Institutes of Health, Bethesda, MD 20892, USA
[e] Institute of Clinical Medicine, University of Oslo, Norway
[f] Department of Emergencies and Critical Care, Oslo University Hospital, Oslo, Norway
[g] The Norwegian Transgenic Center, Institute of Basic Medical Sciences, University of Oslo, Norway

ARTICLE INFO

Keywords:
Plin5
Cardiomyocyte
Lipid droplet
Fatty acid flux
Hypoxia
Glycogen

ABSTRACT

Plin5 is abundantly expressed in the heart where it binds to lipid droplets (LDs) and facilitates physical interaction between LDs and mitochondria. We isolated cardiomyocytes from adult *Plin5*$^{+/+}$ and *Plin5*$^{-/-}$ mice to study the role of Plin5 for fatty acid uptake, LD accumulation, fatty acid oxidation, and tolerance to hypoxia. Cardiomyocytes isolated from *Plin5*$^{-/-}$ mice cultured with oleic acid stored less LDs than *Plin5*$^{+/+}$, but comparable levels to *Plin5*$^{+/+}$ cardiomyocytes when adipose triglyceride lipase activity was inhibited. The ability to oxidize fatty acids into CO_2 was similar between *Plin5*$^{+/+}$ and *Plin5*$^{-/-}$ cardiomyocytes, but *Plin5*$^{-/-}$ cardiomyocytes had a transient increase in intracellular fatty acid oxidation intermediates. After pre-incubation with oleic acids, *Plin5*$^{-/-}$ cardiomyocytes retained a higher content of glycogen and showed improved tolerance to hypoxia compared to *Plin5*$^{+/+}$. In isolated, perfused hearts, deletion of Plin5 had no important effect on ventricular pressures or infarct size after ischemia. Old *Plin5*$^{-/-}$ mice had reduced levels of cardiac triacylglycerides, increased heart weight, and apart from modest elevated expression of mRNAs for beta myosin heavy chain *Myh7* and the fatty acid transporter *Cd36*, other genes involved in fatty acid oxidation, glycogen metabolism and glucose utilization were essentially unchanged by removal of Plin5. Plin5 seems to facilitate cardiac LD storage primarily by repressing adipose triglyceride lipase activity without altering cardiac fatty acid oxidation capacity. Expression of Plin5 and cardiac LD content of isolated cardiomyocytes has little importance for tolerance to acute hypoxia and ischemia, which contrasts the protective role for Plin5 in mouse models during myocardial ischemia.

Abbreviations: ATGL, adipose triglyceride lipase; BDM, 2,3-Butanedione monoxime; BSA, bovine serum albumin; Cpt1a/b, carnitine palmitoyltransferase 1a/b; Fabp3/4, fatty acid binding protein 3/4; FBS, fetal bovine serum; Gapdh, glyceraldehyde 3-phosphate dehydrogenase; Gbe1, glucan (1,4-alpha-) branching enzyme 1; Gyg, glycogenin; Gys1, glycogen synthase 1; Hk1/2, hexokinase 1/2; HR, heart rate; LD, lipid droplet; LDH, lactate dehydrogenase; LVdevP, left ventricular developed pressure; LVEDP, left ventricular end-diastolic pressure; LVSP, left ventricular systolic pressure; Myh6, myosin heavy chain α isoform; Myh7, myosin heavy chain β isoform; Nppa/b, natriuretic peptide type A/B; OA, oleic acid; Pdha1, pyruvate dehydrogenase E1 alpha 1; Pdk4, pyruvate dehydrogenase kinase, isoenzyme 4; Pygm, glycogen phosphorylase; RPP, rate pressure product; Rplp0, ribosomal protein lateral stalk subunit p0; Slc2a1/4, solute carrier family 2 member 1/4 (Glut1/4); TAG, triacylglycerols; TLC, thin layer chromatography; TTC, triphenyl tetrazolium chloride.

* Corresponding author at: Department of Nutrition, Institute of Basic Medical Sciences, Faculty of Medicine, University of Oslo, P.O. Box 1046, Blindern, N-0316 Oslo, Norway.
E-mail address: k.t.dalen@medisin.uio.no (K.T. Dalen).

https://doi.org/10.1016/j.bbalip.2020.158873
Received 21 September 2020; Received in revised form 17 December 2020; Accepted 22 December 2020
Available online 26 December 2020

1. Introduction

Myocardial ischemia and infarction is a leading cause of death worldwide. Cardiac energy metabolism prior to and during acute myocardial ischemia may be important for the outcome and later clinical complications [1–6]. The heart is able to use multiple energy substrates, with substrate preference influenced by various physiological and pathophysiological conditions [7,8]. Normally, 60%–70% of cardiac energy derives from oxidation of fatty acids, while the remaining energy is mainly generated from oxidation of glucose [9,10]. Notably, cardiomyocytes are equipped with reservoirs for these energy substrates. Fatty acids are stored as triacylglycerol (TAG) in lipid droplets (LDs), and glucose is stored as glycogen. During acute myocardial ischemia, low oxygen levels inhibit aerobic fatty acid oxidation for generation of ATP through mitochondrial oxidative phosphorylation. Instead, the ischemic heart generates ATP primarily by glycolysis. Glucosyl units mobilized from glycogen are converted to pyruvate, which is then converted into lactate to regenerate NAD^+ to sustain glycolysis. However, during prolonged hypoxia, the accumulated lactate causes cellular acidification, reduced glycolytic rates, and eventually cell damage and cell death [11].

Cardiomyocytes take up glucose from the circulation, where generated glucose-6-phosphate is converted *via* glucose-1-phosphate into UDP-glucose that serves as building blocks for glycogen synthesis [12]. The final key steps in the glycogen synthesis pathway, and the initial step in the glycogen degradation pathways, are reciprocally regulated by various hormones in tissue-specific manners [13–15]. Liver and muscle serve as the main reservoirs for glycogen stores, which become mobilized during stress, starvation and exercise. During these conditions, myocardium uses fatty acids as the main energy source and the cardiac glycogen is preserved or even increased [16,17]. The physiological/pathological importance of the differently regulated cardiac glycogen storage is unclear.

Circulating fatty acids taken up by cardiomyocytes are incorporated into TAG and stored in LDs to balance intracellular levels of free fatty acids. Formation of new and expansion of existing LD (esterification of lipids) and LD degradation (lipolysis or lipophagy) are tightly regulated processes [18]. These processes are regulated by proteins permanently or transiently recruited to the surface of LDs, such as LD-coating proteins, lipid esterification enzymes, lipolytic factors and autophagosome recruiting proteins [19]. The perilipins constitute a major LD-coating protein family in mammals, consisting of the *Plin*1–5 genes that are expressed in a tissue-specific manner [20]. Of these, Plin5 is unique for mammals [21] and is highly expressed in oxidative tissues rich in mitochondria, such as the myocardium [22–24]. Mice lacking Plin5 have reduced cardiac LD content [25], whereas mice with cardiac-specific Plin5 overexpression have increased cardiac LD content [26,27]. Plin5 facilitates physical interaction between LDs and mitochondria [28]. The significance of this interaction is unclear, but mitochondria interacting with LDs seem to have altered energy metabolism [29].

The role of LDs in ischemic heart disease is unclear. Accumulation of LDs in the myocardium has been observed in the boundary of an infarct area, in failing hearts, and in diabetic cardiomyopathy [30–32]. A few *in vitro* studies suggest that formation of LDs and enhanced TAG turnover in cardiomyocytes may protect against ischemia-reperfusion injury [4,33]. Cardiac overexpression of Plin5 increases LD content in the heart, causing slightly impaired cardiac mitochondrial function without affecting heart function [26]. In contrast, *Plin5*$^{-/-}$ mice with low levels of cardiac LDs have reduced survival after myocardial ischemia [34]. These studies show that cardiac LD storage can be manipulated by interfering with Plin5, but the consequences of such manipulation for cardiac energy metabolism is still unclear. The purpose of this study was to compare fatty acid uptake, LD accumulation, and fatty acid oxidation in cultured Plin5$^{+/+}$ and Plin5$^{-/-}$ cardiomyocytes under normoxic and hypoxic conditions, as well as tolerance to ischemia in *ex vivo* perfused hearts.

2. Materials and methods

2.1. Reagents and materials

Plasticware was obtained from Corning Life Sciences (Tewksbury, MA, US) and Sarstedt (Nümbrecht, Germany). Cell culture reagents and Bodipy 493/503 were obtained from Thermo Fisher Scientific (Waltham, MA, US). 2,3-Butanedione monoxime (BDM), paraformaldehyde and Hoechst 33342 were obtained from Sigma-Aldrich (St. Louis, MO, US). Phalloidin-CF568 conjugate was from Biotium (Fremont, CA, US). [1-^{14}C]-oleic acid and D-[^{14}C(U)]-glucose were from PerkinElmer NEN (Boston, MA, US). Materials for real-time quantitative PCR were obtained from Bio-Rad (Hercules, CA, US).

2.2. Animal experiments

Animal use in this study was approved and registered by the Norwegian Animal Research Authority (Mattilsynet, approvals FOTS ids: #6305, #6922 and #10901) and confirmed to the ARRIVE guidelines and ethical guidelines given in Directive 2010/63/EU of the European Parliament on the protection of animals used for scientific purposes. Mice were housed with a stable light/dark cycle (7 am:7 pm) with 55 ± 5% relative humidity at 22 ± 2 °C with free access to water and rodent chow (#RM3-801190, SDS diets, consisting of 12% calories from fat, 27% from protein, and 61% from carbohydrate). The health status of the animals was monitored quarterly and were absent of all pathogens listed by The Federation of European Laboratory Animal Science Associations (FELASA).

Generation of the *Plin5* model is partially described previously [34]. Construction of the *Plin5* targeting vector started with modifying the FRT sites in the p451 vector [35]. The new p451-Hygro-FRT5 vectror was generated by replacing the Neomycin resistant gene (neo) with the Hygromycin resistant gene (*hph*) followed by site directed mutagenesis of the two FRT sites in the p451-vector. Briefly, the *hph* gene was amplified from a vector (pcDNA5/FRT, Invitrogen), the PCR product digested with *Bsp*HI/*Bcl* I and ligated into *Nco*I/Bcl I digested pL451 vector to generate a Hygromycin resistant gene cassette (p451-Hygro vector). Each FRT site was then sequentially mutated to FRT_5 sites, which will not recombine with wild type FRT sites. The 5-end FRT site was mutated with PCR using the primer combination 5-pL451-FRT_5 and 3-pL451-Hygro, followed by ligation into *Xho*I and *Bcl* I digested p451-Hygro to generate p451-FRT_5-Hygro-FRT. The 3-end FRT site was mutated using the primer combination 5-pL451-Hygro and 3-pL451-FRT_5 followed by ligation into *Bsp*HI/*Bcl* I digested p451-FRT_5-Hygro-FRT to generate p451-FRT_5-Hygro-FRT_5. Since the *hph* gene contains an *Eco*RI site, the cassette might be conveniently excised by *Xho*I/BamHI digestion. The new p451-Hygro-FRT_5 vector was subsequently used to construct the *Plin5* targeting vector using recombineering as described previously [35]. Details regarding construction of the targeting vector, electroporation of embryonic stem (ES) cells, Southern blot screening of ES cells, blastocyst injections, generation of chimera, verification of germline transmission, as well as all primers and oligoes used for Southern screening has been described previously [34].

The above *Plin5* model [34] were crossed with mice expressing Flp [36] to remove the Hygromycin selection cassette (See Supplemental Fig. 1), followed by backcrossing for 10 generations into C57BL/6NRj (Janvier Labs, Le Genest-Saint-Isle, France). Experimental Plin5 wild type (*Plin5*$^{+/+}$) and Plin5 null (*Plin5*$^{-/-}$) animals were from the same breeding colony. For tissue collection, mice were euthanized by cervical dislocation at 8 am – 10 am. For *ex vivo* heart perfusion and cardiomyocyte isolation, an intraperitoneal injection of 50 μg/g body weight sodium pentobarbital solution containing 8 IU/g body weight heparin was given to mice prior to euthanasia by cervical dislocation and collection of hearts. The majority of experiments were performed in

animals at 18–30 weeks of age. The number of animals used is stated for each animal experiment. None of the animals used have been excluded from analysis. In total, 45 *Plin5*$^{+/+}$ and 45 *Plin5*$^{-/-}$ mice were used in these studies.

2.3. Ischemia-reperfusion in ex vivo perfused Langendorff mouse heart

Mice were anesthetized and heparinized as described above. The hearts were quickly isolated, the aorta cannulated, then hearts were connected to a Langendorff system (AD Instruments, NSW, Australia) and retrogradely perfused with Krebs-Henseleit buffer (11.1 mM Glucose, 118.5 mM NaCl, 25 mM $NaHCO_3$, 4.7 mM KCl, 1.2 mM KH_2PO_4, 1.2 mM $MgSO_4$, and 2.4 mM $CaCl_2$) during constant bubbling with 95% O_2/5% CO_2 gas. Perfusion pressure was constant at 70 mmHg and temperature (37 °C) was monitored with a probe inside the right atrium. Heart rate, left ventricular systolic pressure (LVSP) and end-diastolic pressure (LVEDP) were recorded by a pressure transducer connected to a water-filled balloon in the left-ventricle. LVEDP was maintained at 5–10 mm Hg during stabilization. Left ventricular developed pressure (LVdevP = LVSP − LVEDP) and rate pressure product (RPP) were calculated by Labchart 7 software (ADInstruments, Dunedin, New Zealand). Exclusion criteria after 20 min of stabilization were: hearts with LVSP ≤ 60 mmHg; coronary flow ≤ 1 mL/min or ≥ 5 ml/min; heart rate ≤ 220 beats/min; time delay >4 min from heart excision to start of perfusion or irreversible arrhythmias during stabilization. The hearts included were subjected to 35 min of no-flow global ischemia followed by 60 min of reperfusion.

At the end of reperfusion, hearts were sliced (1 mm thick cross sections) and stained with 1% triphenyl tetrazolium chloride (TTC, dissolved in PBS) at 37 °C for 15 min for assessment of infarct size. The five middle slices of the heart were acquired with an Epson Perfection V700 scanner (Epson, Suwa, Japan) and blindly analyzed by Image Analyzer plugin of Science Linker B000 database (Science Linker AS, Oslo, Norway). Infarct size was calculated as average percentage of infarct areas in whole heart sections.

2.4. Isolation and stimulation of cardiomyocytes

Cardiomyocytes were isolated based on the method described by O'Connell et al. [37]. Briefly, mice were anesthetized and heparinized prior to cervical dislocation. Hearts were quickly connected to the perfusion system and perfused at 37 °C for 4 min with constant flow (4 mL/min) of perfusion buffer (120.4 mM NaCl, 14.7 mM KCl, 0.6 mM KH_2PO_4, 0.6 mM Na_2HPO_4, 1.2 mM $MgSO_4$, 10 mM Na-HEPES, 4.6 mM $NaCO_3$, 30 mM taurine, 10 mM 2,3-Butanedione monoxime (BDM) and 5.5 mM glucose, pH 7.0) to flush out blood. Thereafter, the heart was perfusion with 15 mL recirculating digestion buffer (perfusion buffer containing 1.33 mg/mL Collagenase II (#4177, Worthington Biochemical; Lakewood, NJ, US)) to digest extracellular matrix. After 3 min, $CaCl_2$ was added to the digestion buffer to achieve a final concentration of 42 μM, followed by 8 min of digestion. Then hearts were disrupted mechanically with sharp forceps in a six-cm petri dish containing 10 mL buffer A (perfusion buffer supplemented with 10% FBS and 12.5 μM $CaCl_2$) and transferred to a 15 mL conical tube. Cells were dissociated by gently pipetting for 3–4 min. Undigested chunks were removed from the cell suspension, and centrifuged at 20 ×*g* for 3 min to spin down cardiomyocytes. The cardiomyocyte pellet was resuspended in 10 mL buffer A and centrifuged again, followed by gradient reintroduction of calcium by repeating suspension and centrifugation in 10 mL perfusion buffer supplemented with 10% FBS, containing 100 μM (buffer B), 400 μM (buffer C) or 900 μM (buffer D) $CaCl_2$. After calcium reintroduction, cardiomyocytes were resuspended in plating medium (Minimum Essential Medium with Hank's balanced salt solution, supplemented with 10% fetal calf serum, 10 mM BDM, 100 U/mL penicillin and 2 mM glutamine) and seeded in laminin (1 μg/cm^2, #354232, BD Biosciences; East Rutherford, NJ, US) coated multiple well plates (Corning Life Sciences, Tewksbury, MA, US) or 8-well chamber slides (# 94.6170.802, Sarstedt; Nümbrecht, Germany). Cardiomyocytes were allowed to recover and attach for 1–2 h at 37 °C under 2% CO_2. Plating medium was replaced by serum-free short-term medium (Minimum Essential Medium with Hank's balanced salt solution, containing 1 mM BDM, 100 U/mL penicillin and 2 mM glutamine) supplemented with 40 μM bovine serum albumin (BSA, control) or oleic acid (OA) complexed to BSA (100 μM OA: 40 μM BSA, referred as OA in the following), vehicle (DMSO) or 10 μM Agtlistatin (ATGL inhibitor). Depending on downstream analyses, cardiomyocytes were stimulated for 2–20 h and maintained undisturbed at 37 °C under 2% CO_2 and atmospheric O_2 until use.

2.5. Confocal imaging of cardiomyocytes

Cardiomyocytes plated in 8-well chamber slides were incubated with serum-free short-term medium and stimulated with vehicle, BSA, OA, and/or Atglistatin. After 20 h of incubation, cells were washed once with Dulbecco's Phosphate-Buffered Saline, fixed with 4% PFA in 0.1 M phosphate buffer pH 7.4 (PB) for 1 h at room temperature, washed twice with PB and stored in PB containing 0.02% NaN_3 at 4 °C until staining. Cells were washed twice with PB and stained for 20 min at room temperature with PB containing Bodipy 493/503 (1 μM for LDs), Hoechst 33342 (5 μM for nuclei) and CF568 conjugated Phalloidin (1 U/mL for F-actin). After three washes with PB, cells were sealed in mounting medium (#P36965, Thermo Fisher Scientific; Waltham, MA, US) under glass coverslips and stored in the dark at room temperature for 24 h to allow hardening of mounting medium. Images were taken under 20× and 63× objectives on a LSM 710 confocal microscope (Carl Zeiss, Oberkochen, Germany). Microscopy laser and filter settings for all channels were optimized for a representative field and kept constant during image acquisition (Bodipy 493/503: λex = 488 nm, λem = 497–545 nm; Hoechst: λex = 405 nm, λem = 414–465 nm; Phalloidin-CF568: λex = 561 nm, λem = 563–632 nm).

2.6. Hypoxia-reoxygenation in cardiomyocytes and cell damage assessments

Cardiomyocytes plated in 12-well dishes were incubated in serum-free short-term medium containing vehicle, BSA, OA and/or Atglistatin for 16 h. Cells were then exposed to hypoxia by changing to pre-equilibrated hypoxic medium (glucose-free short-term medium, pH 6.4) and incubated in a hypoxia chamber (#856-HYPO, Plas Labs; Lansing, MI, US) at 1% O_2, 5% CO_2, 37 °C for 30 min. Reoxygenation was induced by changing to normoxic pre-equilibrated short-term medium (5.5 mM glucose, pH 7.4) followed by incubation under normoxic condition (2% CO_2, atmospheric O_2, 37 °C) for 20 min. Normoxic control groups were subjected to the same media change intervals but were given pre-equilibrated short-term medium and incubated under normoxic conditions. Conditioned medium was harvested at the end of each step and centrifuged at 3000 ×*g* for 5 min to remove cell debris. Cells were collected with lysis buffer after reoxygenation. Samples were kept at 4 °C and analyzed within 48 h.

To estimate damage of cardiomyocytes, concentration of released lactate dehydrogenase (LDH) was measured with LDH Cytotoxicity Detection Kit (#11644793001, Roche; Mannheim, Germany). Reaction absorbance was measured at 492 nm by a microplate reader (Titertek Multiskan PLUS MK II, Thermo Labsystems, Thermo Fisher Scientific; Waltham, MA, US). Total LDH was calculated as the sum of LDH release during pre-incubation, hypoxia/normoxic control and reoxygenation steps and the remaining LDH in the cell lysate.

2.7. Measuring flux of energy substrates in isolated cardiomyocytes

To monitor the flux of energy substrates in *Plin5*$^{+/+}$ and *Plin5*$^{-/-}$ cardiomyocytes, [1-^{14}C]-oleic acid (OA) and D-[^{14}C(U)]-glucose (both

with activity 1 μCi/mL) were added as tracers to serum-free short-term media. Unlabeled OA or glucose were added to achieve the indicated total (labeled+ unlabeled) substrate concentrations. Cardiomyocytes seeded in four parallel 96-well plates (six parallels for each condition) were given serum-free short-term medium (150 μL/well) and stimulated with BSA (control) or OA (100 μM bound to BSA) in the presence of DMSO (vehicle) or Atglistatin (10 μM). Three plates were incubated in the presence of tracers for 2, 6 or 20 h. The fourth plate was incubated in the absence of tracers for 18 h, then with tracer for 2 h. All plates were mounted with a trapping device (see section below) to capture CO_2 released by the cells during the last 2 h of incubation. At the end of the experiment, the culture media was collected and centrifuged at 3000 ×*g* for 5 min to remove cell debris. Cardiomyocytes were washed once with 0.2% BSA in PBS, followed by two washes with cold PBS to remove membrane bound tracers from the cell surface. Finally, cells were lysed in 100 μL 0.1 M NaOH. Plates containing cell lysates were sealed with parafilm and stored in −20 °C until counting of radioactivity and measurement of proteins. ^{14}C radioactivity in trapped CO_2, cell lysates, acid soluble metabolite fractions and conditioned media was determined to calculate metabolic flux.

Trapping of CO_2.

To measure complete oxidation of OA or glucose, CO_2 released during the last 2 h of incubation was trapped in a filter according to Wensaas et al. [38] with minor modifications. Briefly, a UniFilter-96 GF/B plate (#6005177, PerkinElmer; Shelton, CT, US) was immersed with fresh 1 M NaOH (30 μL/well) and inversely fixed on top of a 96-well plate containing cardiomyocytes. A 96-orifice silicon gasket was placed between the filter plate and 96-well plate to seal the sandwich and separate individual wells. The trapping sandwich was kept sealed for 2 h at 37 °C where released CO_2 was absorbed by the NaOH-immersed filters. After trapping, 30 μl/well of Optiphase supermix scintillation cocktail (#1200–439, PerkinElmer; Shelton, CT, US) was added to the filter plates. Plates were sealed with TopSeal-A PLUS (#6050185, PerkinElmer; Shelton, CT, US) prior to measurement of radioactivity.

2.8. Acid soluble metabolites

To measure acid soluble metabolites, cell lysates (30 μl/well) were transferred to a 96-well microtube plate (#721978202, Sarstedt; Nümbrecht, Germany). To precipitate medium to long chain fatty acids (> C6), fatty acid-free bovine serum albumin (10 μL/well) was mixed with the cell lysate, followed by addition of cold 1 M $HClO_4$ (100 μL/well). The plate was incubated at 4 °C for 30 min and then centrifuged at 3500 ×*g* for 10 min at 4 °C. A fraction of the supernatant (40 μL, containing acid soluble metabolites) was carefully collected without disturbing the precipitate.

2.9. Measurement of radioactivity and calculations

Radioactivity in UniFilter-96 GF/B filter plates (trapped CO_2) was measured after two days with a Packard Top Count Microplate Scintillation Counter (PerkinElmer, Shelton, CT, US). For determination of radioactivity in the media, cell lysates and acid soluble metabolite fractions, two wells were combined (resulting in three replicates for each condition. 40 μL were transferred to a white Barex opaque 96-well microplate (#6005162, PerkinElmer; Shelton, CT, US) and mixed with 120 μL/well Optiphase supermix (#1200–439, PerkinElmer; Shelton, CT, US). Plates were sealed with TopSeal-A PLUS and top-counted for 3 min per well. Specific activity (counts per minute (CPM)/nmol of ^{14}C-labeled or total substrate) was calculated based on measured CPM for unconditioned media. Protein content in cell lysates (20 μL cell lysate) were measured with BCA protein assay kit (#23227, Pierce Biotechnology; Rockford, IL, US). Data for uptake or metabolism of OA and glucose are presented as μmol substrate/L for media, or nmol substrate/mg protein for cell lysates, acid soluble fractions and CO_2.

2.10. Determination of glycogen and triacylglycerol content

Glycogen and TAG content was normalized to protein content. Protein content in homogenates described below was measured with BCA protein assay kit (Pierce, Rockford, IL, US). Glycogen was determined with EnzyChrom Glycogen Assay Kit (# E2GN-100, BioAssay Systems; Hayward, CA, US). Powdered frozen heart tissue (~15 mg) or isolated cardiomyocytes (seeded in 6-well plates, stimulated as described above and washed twice in cold PBS) were harvested in 250 μl glycogen buffer (containing 25 mM citrate and 2.5 g/L NaF, pH 4.2). Samples were transferred to micro tubes containing 10–15 glass beads (~1 mm in diameter) and homogenized using Precellys 24 tissue homogenizer (Bertin Technologies; Montigny-le-Bretonneux, France). The homogenate (100 μL) was centrifuged at 14,000 ×*g* for 5 min to remove debris. Samples (10 μL) or glycogen standards were separately mixed with 90 μL working reagent and incubated at room temperature for 30 min. Fluorescence was measured with BioTek Synergy H1 microplate reader (λex = 530 nm, λem = 585 nm).

Triglyceride content in heart tissue was quantified with thin layer chromatography (TLC). Tissue was homogenized in PBS with glass beads using a Precellys 24 tissue homogenizer (Bertin Technologies; Montigny-le-Bretonneux, France). Total lipids were extracted from the tissue homogenate (120 μg protein, 100 μL) by mixing with 200 μL of chloroform: heptane:methanol (4:3:2, *v*/v) followed by vigorously vortex for 2 × 15 seconds. The liquid phases were separated at room temperature for >15 min prior to centrifugation at 1200 ×*g* for 5 min. The lower organic phase was evaporated under N_2 for 5 min and lipids dissolved in 30 μL chloroform:methanol (2:1, v/v). TLC was performed on silica gel 60 plates (Merck Millipore, Billerica, MA) as described previously [39]. TLC plates were scanned with Epson Perfection V700 scanner (Epson; Suwa, Japan). Images were analyzed with ImageJ and concentrations were calculated against a TAG standard curve run in parallel.

2.11. RNA extraction and gene expression analysis

Total RNA was extracted with NucleoSpin® RNA kit (MACHEREY-NAGEL, GmbH & Co. KG; Düren, Germany). Frozen heart tissue (~10 mg) was powdered, transferred to micro tubes containing 10–15 glass beads and homogenized in RA1 buffer using Precellys 24 tissue homogenizer (Bertin Technologies; Montigny-le-Bretonneux, France). Cultured cardiomyocytes were washed once with PBS before harvested in RA1 lysis buffer. Concentrations and quality of extracted RNA were determined with a Nano-Drop ND-1000 Spectrophotometer (Thermo Scientific; Waltham, MA, US).

Total RNA (300 ng) was reversely transcribed into cDNA with High-Capacity cDNA Reverse Transcription Kit (MultiScribe). Gene-specific regions (70–120 bp) were amplified from cDNA (7.5 ng) with assay primers (100 nM each) and SsoAdvanced™ Universal SYBR® Green Supermix (Bio-Rad; CA, US) on the ABI 7900HT system (10 μL reaction, 95 °C for 3 min, followed by 40 cycles; 95 °C for 10 s and 60 °C for 20 s). Primers (listed in Table 1) were designed using Primer-BLAST software. Ribosomal protein lateral stalk subunit P0 (*Rplp0*) and Glyceraldehyde 3-phosphate dehydrogenase (*Gapdh*) mRNAs were verified to be stably expressed and were used as reference genes for cardiomyocytes and tissues, respectively. All data was analyzed with relative quantification (ΔΔCt method) and was presented as gene expression relative to endogenous controls (2-ΔΔCt).

2.12. Statistics

All data were analyzed with Prism 5 (Graphpad Software; CA, US). Parameters reflecting heart function in Langendorff experiments and glycogen measurements were analyzed with two-way ANOVA with Tukey's post-hoc tests. Two tailed Student's *t*-test was used to analyze remaining data. $p < 0.05$ was defined as significant, while a *p*-value between 0.05 and 0.1 was considered as having a tendency of difference.

Table 1
Primers used for RT-qPCR in this study.

Gene name	Accession	Forward primer	Reverse primer	Product size	Intron length
Cd36	NM_001159557.1	AGGCATTCTCATGCCAGTCG	TGTACACAGTGGTGCCTGTT	119	8174
Cpt1a	NM_013495.2	CCCAGCTGTCAAAGATACCGT	GCTGTCATGCGTTGGAAGTC	84	3807
Cpt1b	NM_009948.2	CCCTCATGGTGAACAGCAACT	GCATTGCCTAGACGGGCTG	85	1095
Fabp3	NM_010174.1	GGACAGCAAGAATTTTGATGACTAC	TTGGTCATGCTAGCCACCTG	78	3440
Fabp4	NM_024406.2	GGGAACCTGGAAGCTTGTCTC	CCACTTTCCTTGTGGCAAAGC	83	2316
Gapdh	NM_001289726.1	GGTCCCAGCTTAGGTTCATCAG	AAATCCGTTCACACCGACCTT	87	1082
Gbe1	NM_028803.4	ATGATTCGTCTCATCACTCACG	CCATTCAGGATGCCCAAACT	81	31,717
Gyg	NM_013755.3	GCATCTGGCTTCTGAGCAA	TTGCCCAGCCACTAAAATATGTA	77	12,395
Gys1	NM_030678.3	TTGGGGTCTTCCCCTCCTAC	GTGGAGATGCTGGGGATGC	82	3183
Hk1	NM_010438.3	GGACCACAGTTGGCGTAGA	CTCAGGGTCTTGTGGAACCG	76	3507
Hk2	NM_013820.3	CTTCCCTTGCCAGCAGAACA	TGACCACATCTTCACCCTCG	95	2651
Myh6	NM_001164171.1	TGCGCATTGAGTTCAAGAAGAT	TGAAGGCCCGAATGTTCCAC	75	2548
Myh7	NM_080728.2	CTGACGCAGGAGAGCATCAT	CAATCCTGGCATTGAGTGCAT	103	1754
Nppa	NM_008725.3	CTTCGGGGGTAGGATTGACA	ATCGACTGCCTTTTCCTCCTT	99	390
Nppb	NM_008726.5	GCTGCTTTGGGCACAAGATA	AGCCAGGAGGTCTTCCTACAA	89	443
Pdha1	NM_008810.3	CGTGGTTTCTGTCACTTGTGTG	CGTAGGGTTTATGCCAGCCT	72	1833
Pdk4	NM_013743.2	AAGATGCTCTGCGACCAGTA	CAATGTGGATTGGTTGGCCTG	91	1858
Plin2	NM_007408.3	GGGCTAGACAGGATGGAGGA	CACATCCTTCGCCCCAGTTA	99	2215
Plin3	NM_025836.3	CGAAGCTCAAGCTGCTATGG	TCACCATCCCATACGTGGAAC	98	1147
Plin4	NM_020568.3	ACCAACTCACAGATGGCAGG	AGGCATCTTCACTGCTGGTC	109	1213
Plin5	NM_001077348.1	GGTGAAGACACCACCCTAGC	CCACCACTCGATTCACCACA	115	568
Pygm	NM_011224.2	GAGTGGAGGACGTGGAAAGG	CCGAAGCTCAGGAATTCGGT	77	3654
Rplp0	NM_007475.5	TGCACTCTCGCTTTCTGGA	GCGCTTGTACCCATTGATGATG	110	907
Slc2a1	NM_011400.3	CTCGGATCACTGCAGTTCGG	CGTAGCGGTGGTTCCATGTT	97	11,636
Slc2a4	NM_009204.2	CGACGGACACTCCATCTGTT	ACATAGCTCATGGCTGGAACC	104	524

Data in graphs are shown as means ± SD, or means ± SEM.

3. Results

3.1. Expression of Plins and storage of lipid droplets in isolated cardiomyocytes

Plin5 is expressed at low levels in most cultured cells [40], which precludes functional mechanistic *in vitro* studies on Plin5 function and its effect on energy metabolism. To evaluate if isolated cardiomyocytes are a suitable model to study the metabolic role of Plin5, we first determined *Plin5* mRNA in *Plin5*$^{+/+}$ and *Plin5*$^{-/-}$ cardiomyocytes maintained in culture for up to 20 h. After isolation and one-hour recovery and attachment to laminin (denoted as 0 h), levels of *Plin5* mRNA in *Plin5*$^{+/+}$ cardiomyocytes were comparable to those of heart tissue (Fig. 1A). This indicates that the cardiomyocyte isolation procedure did not affect *Plin5* mRNA levels. When cardiomyocytes were cultured for 20 h in serum-free media in the presence of BSA, *Plin5* mRNA expression reduced significantly, but were still expression significantly (Fig. 1A). Although increased fatty acid concentrations will often stimulate transcription of *Plin5* [40], addition of physiological levels of OA was unable to maintain *Plin5* mRNA expression in cultured cardiomyocytes. As expected, we confirmed that *Plin5* transcripts were undetectable in either cardiomyocytes or heart tissue from *Plin5*$^{-/-}$ mice.

Plin5 deletion did not influence mRNA levels of Plin-family members *Plin2–4* (Fig. 1A). While culturing cardiomyocytes in the absence of OA for 20 h reduced *Plin2* mRNA levels ~50% compared to heart tissue, incubation with OA increased *Plin2* mRNA levels. *Plin3* mRNA was reduced moderately after 20 h, with minimal effect of OA. *Plin4* mRNA decreased ~80% after 20 h compared to heart tissue, but OA partly attenuated this decrease.

To compare LD storage ability, *Plin5*$^{+/+}$ and *Plin5*$^{-/-}$ cardiomyocytes were stained with Bodipy 493/503, Hoechst 33342 and Phalloidin-CF568 to visualize LDs, nuclei and the myofibrils, respectively. None or very few LDs were visible in *Plin5*$^{+/+}$ or *Plin5*$^{-/-}$ cardiomyocytes cultured without OA (Fig. 1B), regardless of the presence of Atglistatin, an inhibitor of adipose triglyceride lipase (ATGL, the primary triglyceride lipase in heart [41]). When cardiomyocytes were incubated with OA, numerous LDs were observed in *Plin5*$^{+/+}$ cardiomyocytes, whereas *Plin5*$^{-/-}$ cardiomyocytes still contained few LDs (Fig. 1B). However, when OA stimulation was combined with Atglistatin, *Plin5*$^{+/+}$ and *Plin5*$^{-/-}$ cardiomyocytes accumulated comparable levels of LDs, at levels above those observed for cardiomyocytes incubated with OA alone (Fig. 1B). Clearly, Plin5 is required for LD storage in cardiomyocytes. Taken together, isolated cardiomyocytes appear to be a suitable model to study Plin5 function and the importance of LD storage for myocardial metabolism.

Accumulation and utilization of fatty acid and glucose in *Plin5*$^{+/+}$ and *Plin5*$^{-/-}$ cardiomyocytes.

To determine if the presence of cardiac LDs may alter utilization of fatty acids and glucose [39], we studied the metabolic profiles of *Plin5*$^{+/+}$ and *Plin5*$^{-/-}$ cardiomyocytes using ^{14}C-labeled oleic acid and glucose. When cardiomyocytes were incubated with 100 μM OA, the levels of OA in the media declined by ~50% after 20 h of incubation, independent of the Plin5 genotype or the presence of Atglistatin (Fig. 2A). However, compared to *Plin5*$^{+/+}$ cardiomyocytes, *Plin5*$^{-/-}$ cardiomyocytes had reduced intracellular storage of OA (Fig. 2B). The difference in OA accumulation between *Plin5*$^{+/+}$ and *Plin5*$^{-/-}$ cardiomyocytes was already evident after 2 h and stabilized by 6 h. In contrast, when ATGL activity was inhibited, accumulation of OA was similar in *Plin5*$^{+/+}$ and *Plin5*$^{-/-}$ cardiomyocytes and significantly increased compared to cells cultured without Atglistatin (Fig. 2B).

Acid soluble metabolites representing various short (<6 carbons) metabolic intermediates formed during fatty acid oxidation [42,43] are measurements of incompletely oxidized fatty acids. The levels of these metabolites were unchanged from two to 20 h in OA-stimulated *Plin5*$^{+/+}$ cardiomyocytes. In contrast, these metabolites increased transiently in OA-stimulated *Plin5*$^{-/-}$ cardiomyocytes after 2 h and peaked at 6 h (Fig. 2C). The transient increase of acid soluble metabolites was inhibited by Atglistatin. This suggests that incomplete fatty acid oxidation differs between *Plin5*$^{+/+}$ and *Plin5*$^{-/-}$ cardiomyocytes, at least during the early phase of incubation.

We then moved on to study complete oxidation of fatty acids into CO_2. Previous studies determining fatty acid oxidation in cells or tissues lacking or overexpressing Plin5 are not fully conclusive [25,44–48]. In the majority of these studies, $^{14}CO_2$ derived from [1-^{14}C]-fatty acids was measured to calculate the amount of fatty acids completely oxidized into CO_2 [49]. To test if labelling conditions influenced such $^{14}CO_2$ measurements, we pre-incubated cardiomyocytes with OA for 18 h, and then incubated with ^{14}C-OA for 2 h while trapping CO_2. Alternatively,

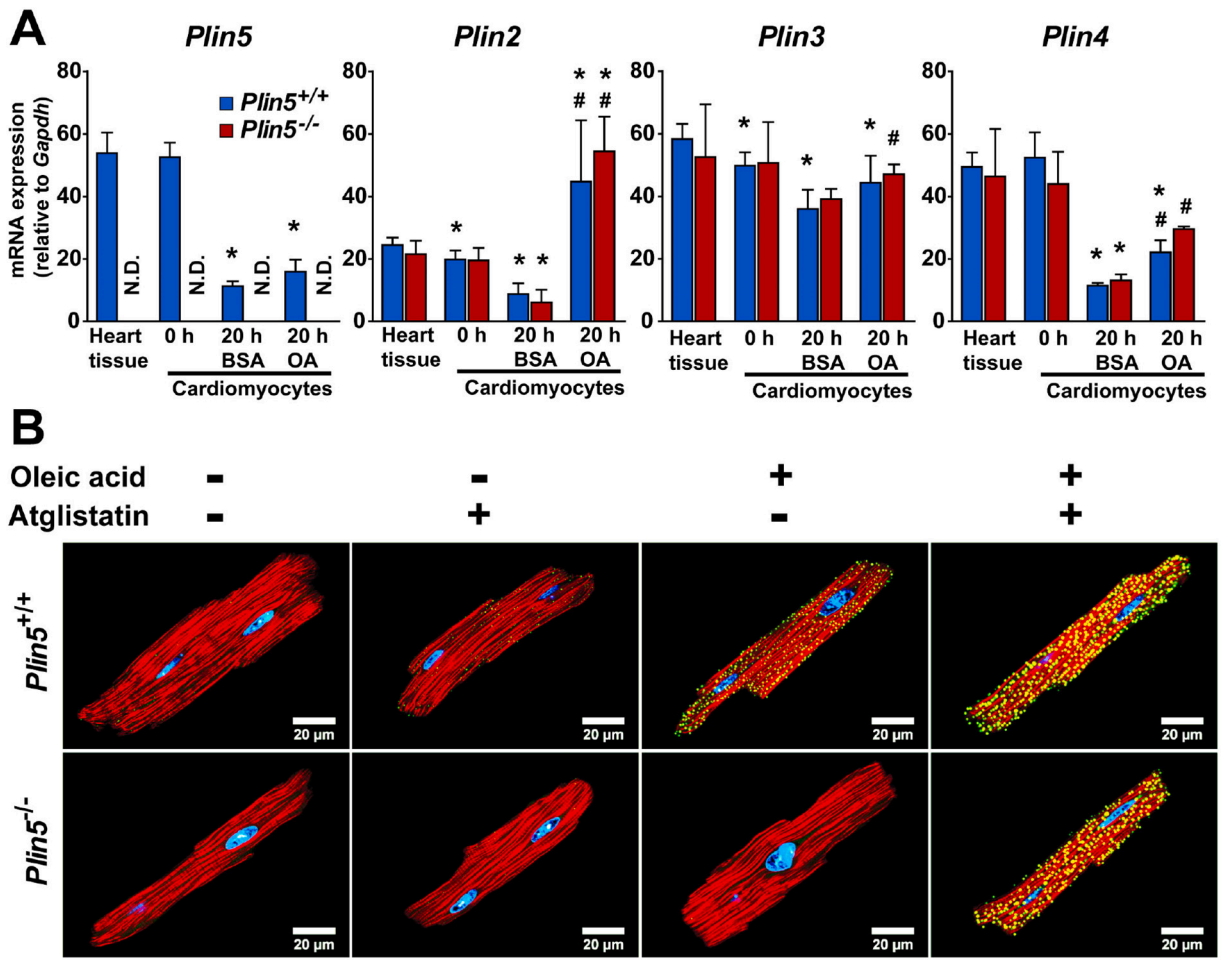

Fig. 1. mRNA expression of *Plin2–5* and LD storage in isolated cardiomyocytes.
Female *Plin5*$^{+/+}$ and *Plin5*$^{-/-}$ mice (16 weeks) with *ad libitum* access to chow were used for extraction of heart tissue or isolation of cardiomyocytes. Cardiomyocytes right after attachment are denoted as 0 h. Cardiomyocytes further incubated for 20 h in the presence of BSA control or 100 μM oleic acid complexed to BSA are denoted as 20 h BSA and 20 h OA, respectively.
A) Relative mRNA expression of *Plin2–5* in heart tissue and isolated cardiomyocytes. mRNA data normalized to *Gapdh* is presented as means ± SD ($n = 4$, *$p < 0.05$ indicate differences compared to heart tissue; #p<0.05 indicate differences between BSA and OA at 20 h of incubation).
B) LD storage in isolated *Plin5*$^{+/+}$ and *Plin5*$^{-/-}$ cardiomyocytes. Cardiomyocytes were incubated for 20 h in media supplemented with BSA or BSA-bound oleic acid (100 μM) in the presence of vehicle (DMSO) or Atglistatin (10 μM). Cells were fixed and stained with Bodipy493/503 to visualize lipid droplets (yellow-green), Hoechst33342 to visualize nuclei (blue), and CF568-Phalloidin to visualize F-actin (red).
Confocal pictures of representative cardiomyocytes taken under a 63× oil immersion objective are shown. Scale bar is 20 μm. Abbreviations: Gapdh, Glyceraldehyde 3-phosphate dehydrogenase; BSA, bovine serum albumin; OA, oleic acid; N.D., not detected.

cardiomyocytes were incubated with ^{14}C-OA for the entire 20 h with trapping of CO_2 during the last 2 h. The captured $^{14}CO_2$ was lower in cardiomyocytes incubated with ^{14}C-OA only for the two last hours (Fig. 2D). This observation suggests that a relatively large fraction of captured CO_2 originates from fatty acids stored in LDs. Furthermore, captured $^{14}CO_2$ was ~50% higher in *Plin5*$^{-/-}$ compared to *Plin5*$^{+/+}$ cardiomyocytes incubated with ^{14}C-OA only for the two last hours, whereas captured $^{14}CO_2$ was similar in *Plin5*$^{+/+}$ and *Plin5*$^{-/-}$ cardiomyocytes incubated with ^{14}C-OA in the 20 h incubation period. These findings demonstrate that labelling conditions, including differences in LD content, may affect the experimental outcome (Fig. 2E), which may explain the controversies regarding the role of Plin5 for fatty acid oxidation. Based on these data, we chose to incubate cardiomyocytes with ^{14}C-OA from 0 to 20 h and trap $^{14}CO_2$ at different time points to determine complete fatty acid oxidation. When cardiomyocytes were incubated in the presence of ^{14}C-OA, calculated total CO_2 production peaked at 4–6 h (Fig. 2F). There was no obvious difference in CO_2 production between *Plin5*$^{+/+}$ and *Plin5*$^{-/-}$ cardiomyocytes at any of the measured time points. Atglistatin had no evident effect on CO_2 production in *Plin5*$^{-/-}$ cardiomyocytes, but CO_2 captured from *Plin5*$^{+/+}$ cardiomyocytes was slightly reduced (Fig. 2F).

We also examined if *Plin5* deletion influenced glucose oxidation. Levels of ^{14}C-glucose in the media were stable during the 20 h of incubation. Cellular accumulation of ^{14}C-glucose was not affected by genotype (Supplemental Fig. 2B). Production of $^{14}CO_2$ derived from ^{14}C-glucose tended to be reduced in *Plin5*$^{+/+}$ and *Plin5*$^{-/-}$ cardiomyocytes in the presence of OA, indicating that fatty acids may repress glucose oxidation. No significant difference in glucose oxidation was noticed between *Plin5*$^{+/+}$ and *Plin5*$^{-/-}$ cardiomyocytes in any groups (Supplemental Fig. 2C), suggesting that Plin5 had no clear effect on glucose oxidation in isolated cardiomyocytes.

Oleic acid increased tolerance to hypoxia in *Plin5*$^{-/-}$ cardiomyocytes.

Previous reports suggest that accumulation of LDs may be protective during hypoxia and ischemia [33,50,51]. We thus studied the effects of hypoxia on cardiomyocytes with or without accumulated LDs. Cell damage was assayed by measurement of released lactate dehydrogenase (LDH) [52]. Under standard normoxic culturing conditions, little

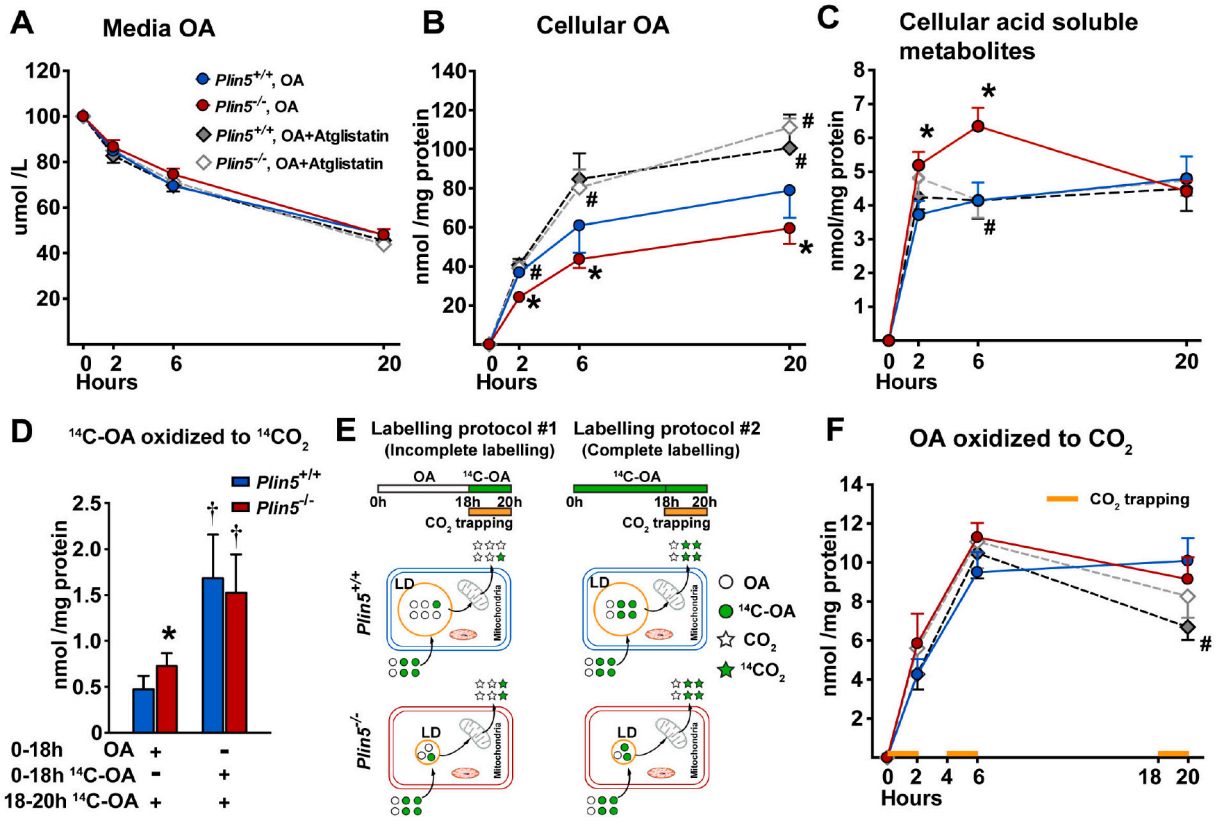

Fig. 2. Metabolism of oleic acid in *Plin5*$^{+/+}$ and *Plin5*$^{-/-}$ cardiomyocytes.
Cardiomyocytes isolated from female *Plin5*$^{+/+}$ and *Plin5*$^{-/-}$ mice (22 weeks females) were incubated with 100 μM OA (unlabeled OA + [1-^{14}C]-OA = 100 μM) bound to BSA in the presence of vehicle (**OA**) or 10 μM Atglistatin (**OA+Atglistatin**). Radioactivity in conditioned media, cell lysate, cellular acid soluble metabolites, and released CO_2 was measured to determine fatty acid flux.
A) OA in conditional media during incubation.
B) Cellular accumulation of OA.
C) Cellular accumulation of acid soluble metabolites, representing incomplete oxidation of OA.
D) [1-^{14}C]-OA oxidized to $^{14}CO_2$ in *Plin5*$^{+/+}$ and *Plin5*$^{-/-}$ cardiomyocytes pre-incubated with either OA or [1-^{14}C]-OA. Cardiomyocytes were incubated with OA for 18 h prior to incubation with [1-^{14}C]-OA for 2 h (protocol #1), or incubated with [1-^{14}C]-OA for 20 h (protocol #2). For both protocols, $^{14}CO_2$ was captured for the last 2 h (18→20 h).
E) The figure illustrates how the LD pool seems to affect $^{14}CO_2$ measurements. Differences in LD content in the presence or absence of Plin5 results in different levels of unlabeled OA *versus* [1-^{14}C]-OA being routed to the mitochondria for oxidation into CO_2.
F) Complete OA oxidation in cardiomyocytes incubated with [1-^{14}C]-OA from time point 0 h (protocol #2). Released $^{14}CO_2$ was captured for 2 h at indicated time points (0 → 2 h, 4 → 6 h, 18 → 20 h) to determine completely oxidized OA. Results are presented as means ± SD in D) and means ± SEM in the rest ($n = 4$–6. *$p < 0.05$ indicate differences between *Plin5*$^{+/+}$ and *Plin5*$^{-/-}$; #$p < 0.05$, indicate differences between vehicle and Atglistatin; †$p < 0.05$ indicate differences between labelling protocols).

difference was observed between *Plin5*$^{+/+}$ and *Plin5*$^{-/-}$ cardiomyocytes, regardless of the OA concentration in the culture media or prevention of lipolysis with Atglistatin (Fig. 3A). Then, *Plin5*$^{+/+}$ and *Plin5*$^{-/-}$ cardiomyocytes were incubated in media supplemented with BSA, OA, or OA combined with Atglistatin for 16 h prior to acute hypoxia followed by reoxygenation. Cell damage was similar in *Plin5*$^{+/+}$ and *Plin5*$^{-/-}$ cardiomyocytes cultured in serum free media, but contradictory to previous studies [25,33,34], pre-incubation with OA reduced damage of *Plin5*$^{-/-}$ cardiomyocytes (Fig. 3B). Hypoxia caused similar damage in *Plin5*$^{+/+}$ and *Plin5*$^{-/-}$ cardiomyocytes incubated with OA in the presence of Atglistatin. Previous studies have linked higher glycogen content to improved outcome after myocardial ischemia [53]. We thus measured glycogen content in cardiomoycytes prior to hypoxic exposure. Glycogen levels were similar in *Plin5*$^{+/+}$ and *Plin5*$^{-/-}$ cardiomyocytes incubated with BSA or Atglistatin for 16 h (Fig. 3C). When incubated with OA, glycogen content was higher in *Plin5*$^{-/-}$ cardiomyocytes compared to *Plin5*$^{+/+}$, whereas levels were significantly reduced in OA and Atglistatin incubated *Plin5*$^{+/+}$ and *Plin5*$^{-/-}$ cardiomyocytes. These results point to alterations in energy sources in OA stimulated *Plin5*$^{-/-}$ cardiomyocytes.

3.2. Deletion of Plin5 did not influence infarct size in isolated, perfused mouse hearts

To follow up our findings in isolated cardiomyocytes, we investigated the effect of Plin5 deletion on ischemia-reperfusion injury in isolated, perfused hearts supplemented with glucose as the main energy substrate. There was no important difference in heart function (LVSP, LVEDP, LVdevP and RPP) or infarct size between isolated, perfused hearts from *Plin5*$^{+/+}$ and *Plin5*$^{-/-}$ mice (Fig. 4A, B, C, E and F). During reperfusion, heart rate was lower in *Plin5*$^{-/-}$ hearts (Fig. 4D), suggesting a chronotropic effect of Plin5 deletion. The less significant role of Plin5 during hypoxia in our *in vitro* cultured cardiomyocyte model (Fig. 3) and *ex vivo* perfused heart model (Fig. 4) are inconsistent with the role of Plin5 during myocardial infarction *in vivo*, where *Plin5*$^{-/-}$ mice have increased infarct size and higher mortality [34,61].

Plin5$^{-/-}$ mice had increased heart weight with age and mild changes in cardiac metabolism.

Heart function of *Plin5*$^{-/-}$ mice may decrease with age [25]. Therefore, we compared hearts from young (15 weeks) and aged (55 weeks) *Plin5*$^{+/+}$ and *Plin5*$^{-/-}$ mice. Body weights were similar at the

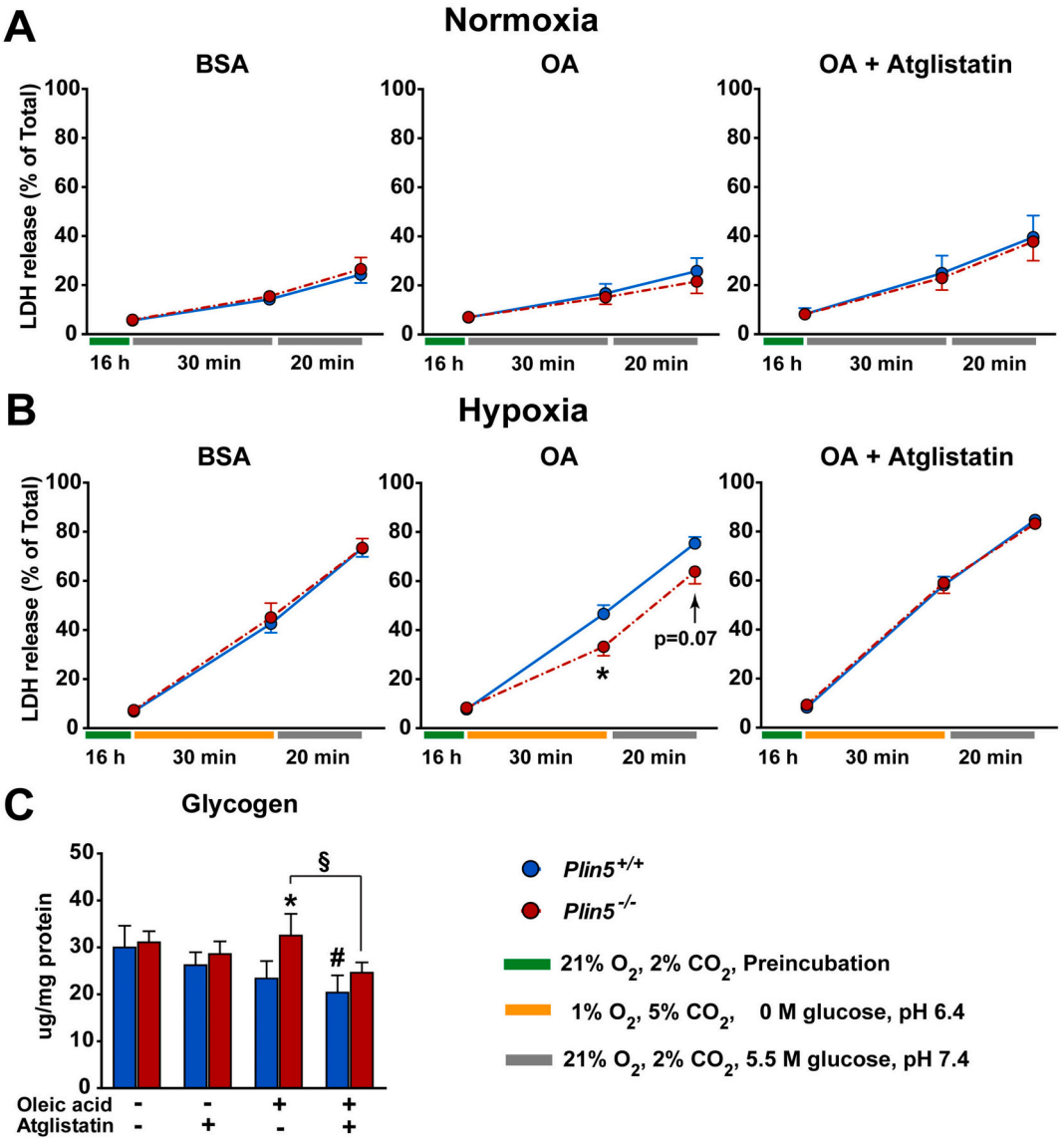

Fig. 3. Incubation with oleic acid alleviates hypoxia induced damage of *Plin5*$^{-/-}$ cardiomyocytes.
Cardiomyocytes were isolated from *Plin5*$^{+/+}$ and *Plin5*$^{-/-}$ mice (16 weeks) and incubated for 16 h in media containing BSA (**BSA**), 100 μM oleic acid (**OA**), or 100 μM OA and 10 μM Atglistatin (**OA + Atglistatin**). Cardiomyocytes were subsequently exposed to normoxia or hypoxia (1% oxygen) for 30 min followed by re-oxygenation for 20 min. Conditioned media were collected before (**16 h**), after normoxia/hypoxia (**30 min**) and after re-oxygenation (**20 min**).
A) LDH released (% of total LDH) from cells exposed to normoxia.
B) LDH released (% of total LDH) from cells exposed to hypoxia.
C) Glycogen content in cardiomyocytes after 16 h of incubation.
Data for LDH measurements is presented as means ± SEM ($n = 6$) and glycogen content as means ± SD ($n = 4$. *$p < 0.05$ indicate differences between *Plin5*$^{+/+}$ and *Plin5*$^{-/-}$ cardiomyocytes, #$p < 0.01$ indicate difference between BSA and other treatments, §$p < 0.05$ indicate difference between OA and OA+Atglistatin).

same age (Fig. 5A). Heart weights of *Plin5*$^{+/+}$ and *Plin5*$^{-/-}$ mice were the same at 15 weeks, whereas the weights of *Plin5*$^{-/-}$ hearts increased about 25% from 15 to 55 weeks of age and were significantly higher than that of *Plin5*$^{+/+}$ hearts at 55 weeks (Fig. 5B). Cardiac expression of myosin heavy chain beta (*Myh7*) mRNA increased with age in both genotypes, and was significantly higher in myocardium of *Plin5*$^{-/-}$ mice compared to *Plin5*$^{+/+}$ at 55 weeks of age (Fig. 5C). Expression of myosin heavy chain alpha (*Myh6*) was unaltered by age or by genotype. mRNAs of *Nppa* and *Nppb,* encoding two natriuretic peptides that usually increase in heart failure, were not different between *Plin5*$^{+/+}$ and *Plin5*$^{-/-}$ hearts, although *Nppb* mRNA levels approximately doubled with age (Fig. 5C).

To compare the cardiac metabolic profile of young and old *Plin5*$^{+/+}$ and *Plin5*$^{-/-}$ mice, we measured the stored energy substrates and expression of selected metabolic genes in myocardium. As expected, cardiac TAG content was lower in *Plin5*$^{-/-}$ mice compared to *Plin5*$^{+/+}$ (Fig. 5D), but increased with age in both genotypes. The variability in cardiac glycogen storage was high between individuals, with no clear difference between ages or genotypes (Fig. 5F). *Plin5*$^{-/-}$ hearts showed minor changes in gene expression associated with fatty acid and glucose metabolisms compared with *Plin5*$^{+/+}$ hearts (Fig. 5E and G). Of note, *Plin5*$^{-/-}$ myocardium had slightly upregulated expression of some genes responsible for fatty acid uptake (*Cd36*) and utilization (*Fabp4*, *Cpt1b*) in old mice, whereas some genes involved in glucose utilization (*Hk2* and *Pdha1*) were mainly elevated in myocardium of young *Plin5*$^{-/-}$ mice. In addition, expression of genes encoding glycogen metabolic enzymes (*Gys1, Gyg,* and *Gbe1*) were slightly elevated in *Plin5*$^{-/-}$ hearts (Fig. 5H). In sum, these modest changes in gene expression would not suggest that

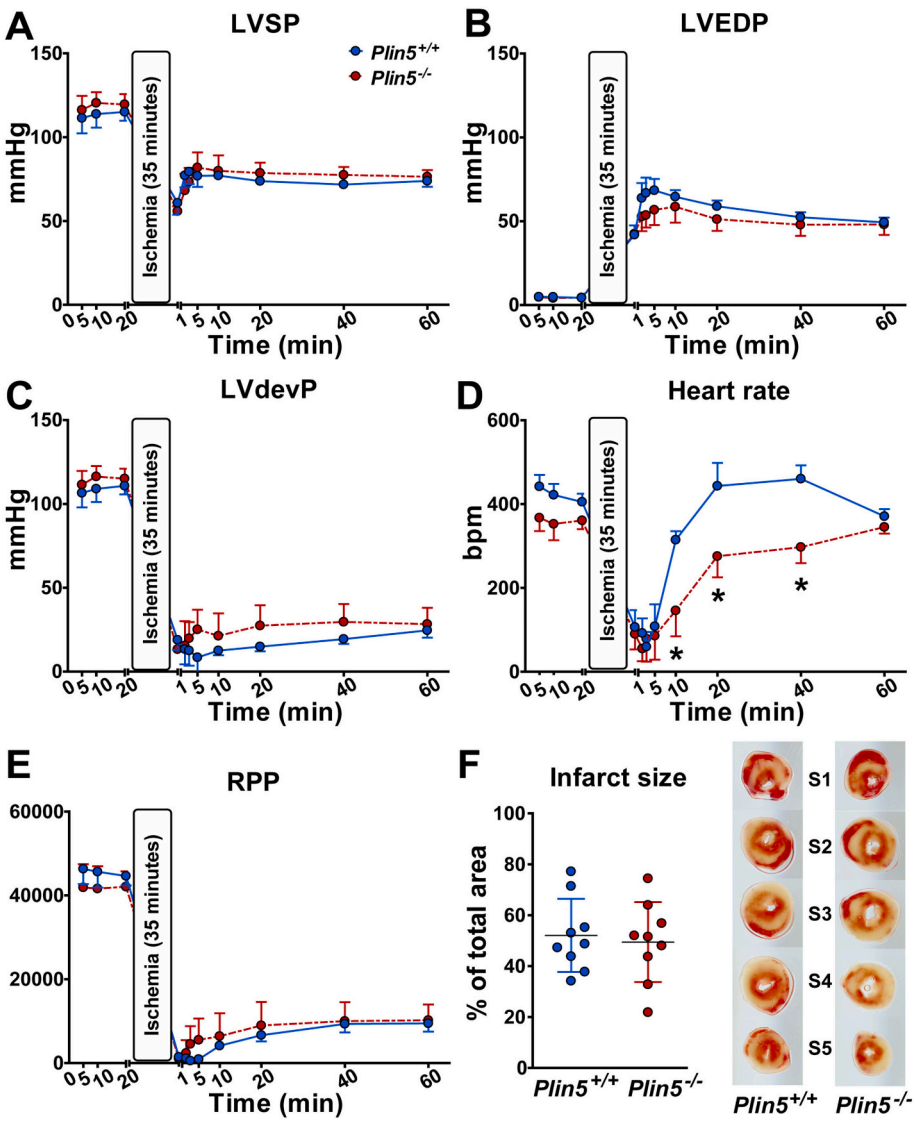

Fig. 4. Heart function and infarct size of *ex vivo* perfused mouse hearts.
Hearts were isolated from male *Plin5*$^{+/+}$ and *Plin5*$^{-/-}$ mice (16 weeks) and retrogradely perfused with Krebs-Henseleit buffer through the aorta. After stabilization for 20 min, hearts were subjected to 35 min of ischemia followed by 60 min of reperfusion. At the end of the reperfusion, heart cross sections (1 mm thick) were stained with triphenyl tetrazolium chloride (TTC) to assess infarct size. **A)** Left ventricular systolic pressure (LVSP). **B)** Left ventricular end-diastolic pressure (LVEDP). **C)** Left ventricular developed pressure (LVdeP = LVSP − LVEDP). **D)** Heart rate. **E)** Rate pressure product (RPP, product of C and D). **F)** Infarct size for *in vitro* perfused *Plin5*$^{+/+}$ and *Plin5*$^{-/-}$ hearts based on TCC staining where viable tissue is shown as red. Each data point gives damage percentage of 5 sections per heart. Sections 1–5 (**S1-S5**, from the heart atrium toward the apex) form one representative for each genotype are shown. Heart function data (**A-E**) is presented as means ± SEM, whereas infarct size (**F**) is presented as means ± SD ($n = 9$. $^*p < 0.05$ indicate differences between *Plin5*$^{+/+}$ and *Plin5*$^{-/-}$ hearts).

altered transcriptional signaling remodels myocardium fatty acid and glycolytic pathways to a large degree. This is in line with unaltered glucose and fatty acid metabolism measured in cultured cardiomyocytes.

4. Discussion

Plin5 is highly expressed in myocardium and is the dominant lipid droplet binding protein in the heart [22–24]. Whole hearts and cardiomyocytes isolated from *Plin5*$^{-/-}$ mice store less LDs, especially after exposure to elevated levels of fatty acids [25,34,46,54], whereas cardiac Plin5 overexpression increases LD content [26,27,46]. In the present study, we compared the metabolic properties of *Plin5*$^{+/+}$ and *Plin5*$^{-/-}$ cardiomyocytes. We showed that *Plin5*$^{-/-}$ cardiomyocytes stored normal levels of LDs when ATGL activity was inhibited. Lack of Plin5 in cardiomyocytes did not affect the complete oxidation of OA into CO_2, but transiently increased intermediate OA metabolites. *Plin5*$^{-/-}$ cardiomyocytes pre-incubated with OA maintained more glycogen and were more tolerant to hypoxia. The heart weight and cardiac *Myh7* mRNA expression increased with age in *Plin5*$^{-/-}$ mice, whereas expression of genes important for glucose and fatty acid metabolism was mostly unaltered. Taken together, our investigation complements previous studies on Plin5 and supports an important role of Plin5 for cardiac LD storage.

Plin5 overexpression increases cardiac LD content [26,27] whereas Plin5 deletion reduces LD storage [25]. In agreement with previous findings, we observed that OA-stimulated LD storage was significantly reduced in *Plin5*$^{-/-}$ cardiomyocytes. Impaired storage of OA and LDs in *Plin5*$^{-/-}$ cardiomyocytes were completely restored by inhibiting ATGL, the key enzyme of cardiac TAG lipolysis [55]. This is in agreement with other reports showing that Plin5 interacts with ATGL and its co-activator alpha-beta hydrolase domain-containing 5 to regulate lipolytic rate [56,57]. Other studies have suggested that altered fatty acid uptake may contribute to the reduced LD levels in *Plin5*$^{-/-}$ hearts. Uptake of palmitic acid is reduced in hearts of *Plin5*$^{-/-}$ mice [34] and the same is reported for hepatocytes of liver-specific *Plin5*$^{-/-}$ mice [44]. Although altered fatty acid uptake may play a role, our results suggest that enhanced lipolysis in the lack of Plin5 is the main factor resulting in the depleted LD storage in cardiomyocytes.

A signal sequence in the C-terminus of Plin5 facilitates physical binding between LDs and mitochondria [28]. This binding seems unique for Plin5 in the Plin family. Due to the relatively restricted expression of Plin5 in oxidative tissues [22–24], Plin5 was initially hypothesized to facilitate fatty acid flux into mitochondria to fuel fatty acid oxidation [58]. A more recent study, however, suggests that Plin5-mediated binding of LDs with mitochondria may provide ATP for the synthesis

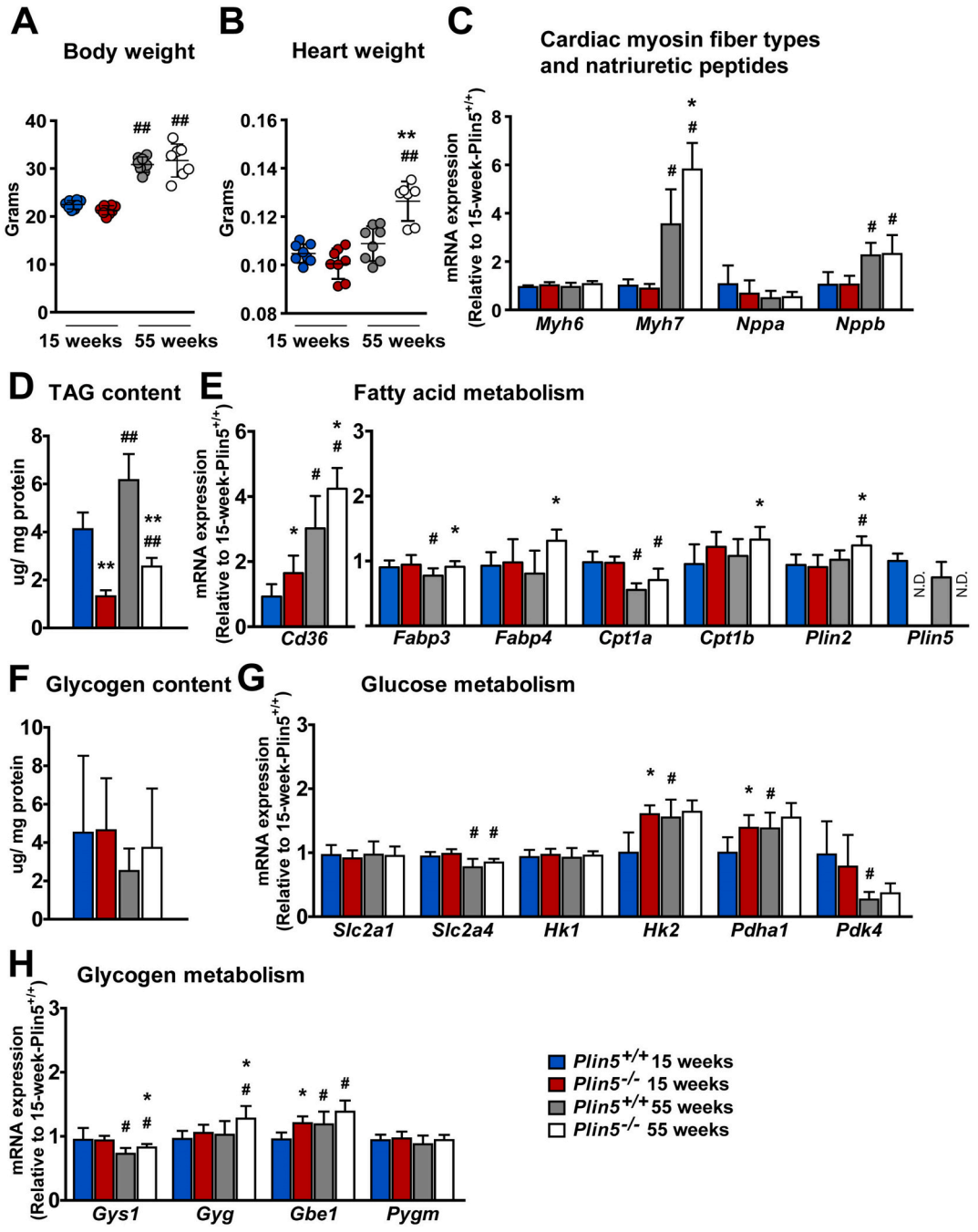

Fig. 5. *Plin5*$^{-/-}$ mice have increased heart weight with age but mild changes in cardiac metabolism

Female *Plin5*$^{+/+}$ and *Plin5*$^{-/-}$ mice (15 and 55 weeks) with *ad libitum* access to chow were analyzed to address differences in heart with aging. **A**) Body weight. **B**) Heart weight. **C**) Expression of mRNAs encoding selected myofiber types and natriuretic peptides. **D)** Cardiac triacylglycerol (TAG) content. **E)** Relative expression of genes involved in fatty acid metabolism. **F)** Cardiac glycogen content. **G)** Relative expression of genes involved in glucose metabolism. **H)** Relative expression of genes involved in glycogen metabolism.

Gene expressions are normalized to the expression of *Rplp0* and are presented as means ± SD relative to expression in 15-weeks *Plin5*$^{+/+}$ heart ($n = 7$–8. $^{*}p < 0.05$, $^{**}p < 0.005$ indicate differences between *Plin5*$^{+/+}$ and *Plin5*$^{-/-}$; $\#p < 0.05$, $\#\#p < 0.005$ indicate differences with age). Abbreviations: Cd36, CD36 molecule; Cpt1a, carnitine palmitoyltransferase 1a; Cpt1b, carnitine palmitoyltransferase 1b; Fabp3, fatty acid binding protein 3; Fabp4, fatty acid binding protein 4; Gbe1, glucan (1,4-alpha-) branching enzyme 1; Gyg, glycogenin; Gys1, glycogen synthase 1; Hk1, hexokinase 1; Hk2, hexokinase 2; Myh6, Myosin heavy chain α isoform; Myh7, Myosin heavy chain β isoform; Nppa, natriuretic peptide type A; Nppb, natriuretic peptide type B; Pdha1, pyruvate dehydrogenase E1 alpha 1; Pdk4, pyruvate dehydrogenase kinase, isoenzyme 4; Pygm, glycogen phosphorylase; Slc2a1, solute carrier family 2 member 1 (Glut1); Slc2a4, solute carrier family 2 member 4 (Glut4); N.D., not detected.

of core lipids to expand LDs [29]. Furthermore, in metabolic flux assays, expression of Plin5 is reported to enhance [44,45], reduce [25,46,47], or have no effect [48] on fatty acid oxidation. The role of Plin5 for fatty acid oxidation is therefore unclear and debated. The discrepant observations may be caused by variations in cell types, the fatty acids used, or other experimental conditions. In metabolic flux assays using radioactive tracers, measured $^{14}CO_2$ is used to estimate total CO_2 production [59]. We compared two labelling protocols to estimate fatty acid

oxidation rate in cardiomyocytes. The production of $^{14}CO_2$ in *Plin5*$^{+/+}$ and *Plin5*$^{-/-}$ cardiomyocytes was similar after pre-labelling with ^{14}C-OA for 18 h. In contrast, production of $^{14}CO_2$ was higher in *Plin5*$^{-/-}$ cardiomyocytes after incubation with unlabeled OA for 18 h. Such observations suggest that the experimental design is decisive for interpretation of oxidative measurements, and may explain the controversy regarding the role of Plin5 for fatty acid oxidation. It is tempting to speculate that genotype-driven differences in intracellular LD levels prior to ^{14}C metabolic tracing experiments influence such measurements. In our study, a higher fraction of unlabeled OA released from LDs in OA pre-incubated *Plin5*$^{+/+}$ cardiomyocytes seems to compete with the newly added ^{14}C-OA as a substrate for fatty acid oxidation, resulting in reduced production of $^{14}CO_2$ compared to levels measured for *Plin5*$^{-/-}$ cardiomyocytes. Furthermore, we observed a transient increase in fatty acid metabolic intermediates (acid soluble metabolites) in *Plin5*$^{-/-}$ cardiomyocytes during the first few hours of OA-incubation. These findings are in agreement with earlier views suggesting that the presence of Plin5 reduces LD turnover [60]. Overall, our metabolic flux assays suggest that deletion of Plin5 in cardiomyocytes may result in a disturbed fatty acid β-oxidation, but do not affect the downstream capacity of mitochondrial oxidative phosphorylation and CO_2 production. This conclusion is supported by examination of young and old *Plin5*$^{+/+}$ and *Plin5*$^{-/-}$ mice, where we observed essentially no obvious difference in the expression of genes important for glucose and fatty acid oxidation between *Plin5*$^{+/+}$ and *Plin5*$^{-/-}$ hearts.

Mice lacking Plin5 in all tissues have increased infarct size and higher mortality following *in vivo* myocardial infarction [34,61]. However, systemic alterations caused by Plin5 deletion in other tissues may contribute to the altered cardiac metabolism, heart function and susceptibility to ischemia/hypoxia [47,62,63], confounding our understanding on the cardiac-specific role of Plin5 *per se* during myocardial ischemia. Alternatively, factors external to cardiomyocytes and produced independently of Plin5 may influence hearts of *Plin5*$^{+/+}$ and *Plin5*$^{-/-}$ mice differentially. Our *ex vivo* heart and isolated cardiomyocyte models have such systemic interactions excluded [37]. The infarct size was similar in *ex vivo* perfused hearts from *Plin5*$^{+/+}$ and *Plin5*$^{-/-}$ mice. In this model, it might be that the *Plin5*$^{-/-}$ phenotype was masked by the absence of exogenous fatty acids. This result is in contrast to the previously reported protective effects of Plin5 during cardiac ischemia *in vivo* [34,61]. Still, when isolated cardiomyocytes were pre-treated with OA, we did observe protective effects in *Plin5*$^{-/-}$ cardiomyocytes during hypoxia.

It has been suggested that LDs may protect cardiomyocytes from ischemia-reperfusion injury by preventing excessive cytosolic levels of free fatty acids and Ca^{2+} [33]. However, OA stimulated LD-deficient *Plin5*$^{-/-}$ cardiomyocytes had less damage compared to OA stimulate LD-rich *Plin5*$^{+/+}$ cardiomyocytes. Thus, our results are not consistent with a simple protective role for accumulated LDs in cardiomyocytes prior to hypoxia. Instead, we speculate that factors other than just LD content may have influenced hypoxia-induced damage in cardiomyocytes. During hypoxia, cardiomyocytes must rely on anaerobic metabolism for ATP production. This is achieved through conversion of glucose or other energy substrates into pyruvate, followed by conversion of pyruvate to lactate [53,64]. Therefore, the glycogen content of cardiomyocytes and the ability to use alternative energy sources are important for cell viability during hypoxia. Metabolic flux assays suggest that glucose accumulation and glucose oxidation were similar in isolated *Plin5*$^{+/+}$ and *Plin5*$^{-/-}$ cardiomyocytes. Still, a higher glycogen content was detected in *Plin5*$^{-/-}$ cardiomyocytes exposed to OA. This suggests that hypoxia-induced damage might be reduced by preservation of the glycogen storage in *Plin5*$^{-/-}$ cardiomyocytes.

Previous studies suggest that heart function declines with age in *Plin5*$^{-/-}$ mice [25]. In our study, heart weight and cardiac *Myh7* mRNA levels increased slightly in aged *Plin5*$^{-/-}$ mice. Expression of *Nppa* and *Nppb* mRNAs, two biomarkers of heart failure [65–67], was not affected by genotype. Expression of certain genes important for fatty acid and glucose oxidation were altered by age, but were essentially similarly expressed in *Plin5*$^{+/+}$ and *Plin5*$^{-/-}$ hearts. Although no detailed investigation on heart function was performed in young and old mice, enlargement of the *Plin5*$^{-/-}$ heart with age seems not to involve altered capacity to metabolize glucose or fatty acids. Plin5 deficiency seems to cause myocardial remodeling that may influence heart failure with age, but based on other reports, this seems to depend on cardiac stress levels [34,61].

In summary, our results suggest that Plin5 deficient cardiomyocytes have an impaired ability to store LDs due to enhanced ATGL catalyzed lipolysis. The reduced LD storage decreased the capacity to sequester cytosolic fatty acids in *Plin5*$^{-/-}$ cardiomyocytes, but without significantly changing the rate of complete fatty acid oxidation. Accumulation of cardiac LDs *per se* does not seem to have a major protective effect on hypoxic damage in isolated cardiomyocytes. Although pretreatment with OA preserved glycogen storage and improved tolerance to hypoxia in *Plin5*$^{-/-}$ cardiomyocytes, our results underscore a complex interrelationship among heart and other tissues in the role of LD and glycogen storage/metabolism during ischemia.

Declaration of competing interest

The authors declare that they have no conflicts of interest with the contents of this article.

Acknowledgement

The authors thank engineers Ingunn Jermstad and Shasta Khan at the Norwegian Transgenic Centre for technical assistance and members of the Dalen laboratory and the Molecular Nutrition Unit at the Department of Nutrition for scientific discussions. This work was supported by grants from South-Eastern Health Authorities, the Medical Faculty at University of Oslo, Henning and Johan Throne-Holst Foundation, Aktieselskabet Freia Chocolade Fabrik's Medical Foundation, Anders Jahre's Foundation, and the Intramural Research Program of the National Institutes of Health (NIH), the National Institute of Diabetes and Digestive and Kidney Diseases (NIDDK).

Appendix A. Supplementary data

Supplementary data to this article can be found online at https://doi.org/10.1016/j.bbalip.2020.158873.

References

[1] W. Wang, G.D. Lopaschuk, Metabolic therapy for the treatment of ischemic heart disease: reality and expectations, Expert. Rev. Cardiovasc. Ther. 5 (2007) 1123–1134.
[2] J.D. Horowitz, Y.Y. Chirkov, J.A. Kennedy, A.L. Sverdlov, Modulation of myocardial metabolism: an emerging therapeutic principle, Curr. Opin. Cardiol. 25 (2010) 329–334.
[3] E. Liepinsh, M. Makrecka, J. Kuka, E. Makarova, R. Vilskersts, H. Cirule, E. Sevostjanovs, S. Grinberga, O. Pugovics, M. Dambrova, The heart is better protected against myocardial infarction in the fed state compared to the fasted state, Metab. Clin. Exp. 63 (2014) 127–136.
[4] S.C. Kolwicz Jr., L. Liu, I.J. Goldberg, R. Tian, Enhancing cardiac triacylglycerol metabolism improves recovery from ischemic stress, Diabetes 64 (2015) 2817–2827.
[5] W. Bouida, K. Beltaief, M.A. Msolli, N. Bzeouich, A. Sekma, M. Echeikh, M. Mzali, H. Boubaker, M.H. Grissa, R. Boukef, M. Hassine, Z. Dridi, A. Belguith, F. Najjar, I. Khochtali, S. Nouira, One-year outcome of intensive insulin therapy combined to glucose-insulin-potassium in acute coronary syndrome: a randomized controlled study, Journal of the American Heart Association 6 (2017).
[6] E.S.S. Hansen, R.S. Tougaard, T.S. Norlinger, E. Mikkelsen, P.M. Nielsen, L. B. Bertelsen, H.E. Botker, H.S. Jorgensen, C. Laustsen, Imaging porcine cardiac substrate selection modulations by glucose, insulin and potassium intervention: a hyperpolarized [1-(13) C]pyruvate study, NMR in Biomedicine 30 (2017).
[7] H. Taegtmeyer, C.R. Wilson, P. Razeghi, S. Sharma, Metabolic energetics and genetics in the heart, Ann. N. Y. Acad. Sci. 1047 (2005) 208–218.
[8] Q.G. Karwi, G.M. Uddin, K.L. Ho, G.D. Lopaschuk, Loss of metabolic flexibility in the failing heart, Frontiers in cardiovascular medicine 5 (2018) 68.

[9] G.J. van der Vusse, J.F. Glatz, H.C. Stam, R.S. Reneman, Fatty acid homeostasis in the normoxic and ischemic heart, Physiol. Rev. 72 (1992) 881–940.
[10] G.D. Lopaschuk, J.R. Ussher, C.D. Folmes, J.S. Jaswal, W.C. Stanley, Myocardial fatty acid metabolism in health and disease, Physiol. Rev. 90 (2010) 207–258.
[11] D.K. Das, R.M. Engelman, J.A. Rousou, R.H. Breyer, Aerobic vs anaerobic metabolism during ischemia in heart muscle, Ann. Chir. Gynaecol. 76 (1987) 68–76.
[12] F. Rajas, A. Gautier-Stein, G. Mithieux, Glucose-6 phosphate, a central hub for liver carbohydrate metabolism, Metabolites 9 (2019).
[13] E. Kokubun, S.M. Hirabara, J. Fiamoncini, R. Curi, H. Haebisch, Changes of glycogen content in liver, skeletal muscle, and heart from fasted rats, Cell Biochem. Funct. 27 (2009) 488–495.
[14] P.J. Roach, A.A. Depaoli-Roach, T.D. Hurley, V.S. Tagliabracci, Glycogen and its metabolism: some new developments and old themes, The Biochemical journal 441 (2012) 763–787.
[15] C. Prats, T.E. Graham, J. Shearer, The dynamic life of the glycogen granule, J. Biol. Chem. 293 (2018) 7089–7098.
[16] G. Evans, The glycogen content of the rat heart, J. Physiol. 82 (1934) 468–480.
[17] C.A. Schneider, V.T. Nguyễn, H. Taegtmeyer, Feeding and fasting determine postischemic glucose utilization in isolated working rat hearts, Am. J. Phys. 260 (1991) H542–H548.
[18] J.A. Olzmann, P. Carvalho, Dynamics and functions of lipid droplets, Nat. Rev. Mol. Cell Biol. 20 (2019) 137–155.
[19] L. Yang, Y. Ding, Y. Chen, S. Zhang, C. Huo, Y. Wang, J. Yu, P. Zhang, H. Na, H. Zhang, Y. Ma, P. Liu, The proteomics of lipid droplets: structure, dynamics, and functions of the organelle conserved from bacteria to humans, J. Lipid Res. 53 (2012) 1245–1253.
[20] A.R. Kimmel, C. Sztalryd, The Perilipins: major cytosolic lipid droplet-associated proteins and their roles in cellular lipid storage, mobilization, and systemic homeostasis, Annu. Rev. Nutr. 36 (2016) 471–509.
[21] J.G. Granneman, V.A. Kimler, H. Zhang, X. Ye, X. Luo, J.H. Postlethwait, R. Thummel, Lipid droplet biology and evolution illuminated by the characterization of a novel perilipin in teleost fish, eLife 6 (2017).
[22] N.E. Wolins, B.K. Quaynor, J.R. Skinner, A. Tzekov, M.A. Croce, M.C. Gropler, V. Varma, A. Yao-Borengasser, N. Rasouli, P.A. Kern, B.N. Finck, P.E. Bickel, OXPAT/PAT-1 is a PPAR-induced lipid droplet protein that promotes fatty acid utilization, Diabetes 55 (2006) 3418–3428.
[23] T. Yamaguchi, S. Matsushita, K. Motojima, F. Hirose, T. Osumi, MLDP, a novel PAT family protein localized to lipid droplets and enriched in the heart, is regulated by peroxisome proliferator-activated receptor alpha, J. Biol. Chem. 281 (2006) 14232–14240.
[24] K.T. Dalen, T. Dahl, E. Holter, B. Arntsen, C. Londos, C. Sztalryd, H.I. Nebb, LSDP5 is a PAT protein specifically expressed in fatty acid oxidizing tissues, Biochim. Biophys. Acta 1771 (2007) 210–227.
[25] K. Kuramoto, T. Okamura, T. Yamaguchi, T.Y. Nakamura, S. Wakabayashi, H. Morinaga, M. Nomura, T. Yanase, K. Otsu, N. Usuda, S. Matsumura, K. Inoue, T. Fushiki, Y. Kojima, T. Hashimoto, F. Sakai, F. Hirose, T. Osumi, Perilipin 5, a lipid droplet-binding protein, protects heart from oxidative burden by sequestering fatty acid from excessive oxidation, J. Biol. Chem. 287 (2012) 23852–23863.
[26] H. Wang, U. Sreenivasan, D.W. Gong, K.A. O'Connell, E.R. Dabkowski, P. A. Hecker, N. Ionica, M. Konig, A. Mahurkar, Y. Sun, W.C. Stanley, C. Sztalryd, Cardiomyocyte-specific perilipin 5 overexpression leads to myocardial steatosis and modest cardiac dysfunction, J. Lipid Res. 54 (2013) 953–965.
[27] N.M. Pollak, M. Schweiger, D. Jaeger, D. Kolb, M. Kumari, R. Schreiber, S. Kolleritsch, P. Markolin, G.F. Grabner, C. Heier, K.A. Zierler, T. Rulicke, R. Zimmermann, A. Lass, R. Zechner, G. Haemmerle, Cardiac-specific overexpression of perilipin 5 provokes severe cardiac steatosis via the formation of a lipolytic barrier, J. Lipid Res. 54 (2013) 1092–1102.
[28] H. Wang, U. Sreenivasan, H. Hu, A. Saladino, B.M. Polster, L.M. Lund, D.W. Gong, W.C. Stanley, C. Sztalryd, Perilipin 5, a lipid droplet-associated protein, provides physical and metabolic linkage to mitochondria, J. Lipid Res. 52 (2011) 2159–2168.
[29] I.Y. Benador, M. Veliova, K. Mahdaviani, A. Petcherski, J.D. Wikstrom, E.A. Assali, R. Acin-Perez, M. Shum, M.F. Oliveira, S. Cinti, C. Sztalryd, W.D. Barshop, J. A. Wohlschlegel, B.E. Corkey, M. Liesa, O.S. Shirihai, Mitochondria bound to lipid droplets have unique bioenergetics, composition, and dynamics that support lipid droplet expansion, Cell Metabolism 27 (2018) 869–885, e866.
[30] Y. Ichikawa, K. Kitagawa, S. Chino, M. Ishida, K. Matsuoka, T. Tanigawa, T. Nakamura, T. Hirano, K. Takeda, H. Sakuma, Adipose tissue detected by multislice computed tomography in patients after myocardial infarction, J. Am. Coll. Cardiol. Img. 2 (2009) 548–555.
[31] J.M. McGavock, I. Lingvay, I. Zib, T. Tillery, N. Salas, R. Unger, B.D. Levine, P. Raskin, R.G. Victor, L.S. Szczepaniak, Cardiac steatosis in diabetes mellitus: a 1H-magnetic resonance spectroscopy study, Circulation 116 (2007) 1170–1175.
[32] S. Sharma, J.V. Adrogue, L. Golfman, I. Uray, J. Lemm, K. Youker, G.P. Noon, O. H. Frazier, H. Taegtmeyer, Intramyocardial lipid accumulation in the failing human heart resembles the lipotoxic rat heart, FASEB journal: official publication of the Federation of American Societies for Experimental Biology 18 (2004) 1692–1700.
[33] I. Barba, L. Chavarria, M. Ruiz-Meana, M. Mirabet, E. Agullo, D. Garcia-Dorado, Effect of intracellular lipid droplets on cytosolic Ca2+ and cell death during ischaemia-reperfusion injury in cardiomyocytes, J. Physiol. 587 (2009) 1331–1341.
[34] C. Drevinge, K.T. Dalen, M.N. Mannila, M.S. Tang, M. Stahlman, M. Klevstig, A. Lundqvist, I. Mardani, F. Haugen, P. Fogelstrand, M. Adiels, J. Asin-Cayuela, C. Ekestam, J.R. Gadin, Y.K. Lee, H. Nebb, S. Svedlund, B.R. Johansson, L. M. Hulten, S. Romeo, B. Redfors, E. Omerovic, M. Levin, L.M. Gan, P. Eriksson, L. Andersson, E. Ehrenborg, A.R. Kimmel, J. Boren, M.C. Levin, Perilipin 5 is protective in the ischemic heart, Int. J. Cardiol. 219 (2016) 446–454.
[35] P. Liu, N.A. Jenkins, N.G. Copeland, A highly efficient recombineering-based method for generating conditional knockout mutations, Genome Res. 13 (2003) 476–484.
[36] F.W. Farley, P. Soriano, L.S. Steffen, S.M. Dymecki, Widespread recombinase Expression Using FLPeR (flipper) Mice vol. 28, Genesis, New York, N.Y., 2000, pp. 106–110.
[37] T.D. O'Connell, M.C. Rodrigo, P.C. Simpson, Isolation and culture of adult mouse cardiac myocytes, Methods in Molecular Biology (Clifton, N.J.) 357 (2007) 271–296.
[38] A.J. Wensaas, A.C. Rustan, K. Lovstedt, B. Kull, S. Wikstrom, C.A. Drevon, S. Hallen, Cell-based multiwell assays for the detection of substrate accumulation and oxidation, J. Lipid Res. 48 (2007) 961–967.
[39] Y.Z. Feng, J. Lund, Y. Li, I.K. Knabenes, S.S. Bakke, E.T. Kase, Y.K. Lee, A. R. Kimmel, G.H. Thoresen, A.C. Rustan, K.T. Dalen, Loss of perilipin 2 in cultured myotubes enhances lipolysis and redirects the metabolic energy balance from glucose oxidation towards fatty acid oxidation, J. Lipid Res. 58 (2017) 2147–2161.
[40] C. Bindesboll, O. Berg, B. Arntsen, H.I. Nebb, K.T. Dalen, Fatty acids regulate perilipin5 in muscle by activating PPARdelta, J. Lipid Res. 54 (2013) 1949–1963.
[41] N. Mayer, M. Schweiger, M. Romauch, G.F. Grabner, T.O. Eichmann, E. Fuchs, J. Ivkovic, C. Heier, I. Mrak, A. Lass, G. Hofler, C. Fledelius, R. Zechner, R. Zimmermann, R. Breinbauer, Development of small-molecule inhibitors targeting adipose triglyceride lipase, Nat. Chem. Biol. 9 (2013) 785–787.
[42] V.W. van Hinsbergh, J.H. Veerkamp, H.T. van Moerkerk, Palmitate oxidation by rat skeletal muscle mitochondria. Comparison of polarographic and radiochemical experiments, Arch. Biochem. Biophys. 190 (1978) 762–771.
[43] V.W. van Hinsbergh, J.H. Veerkamp, H.T. van Moerkerk, An accurate and sensitive assay of long-chain fatty acid oxidation in human skeletal muscle, Biochemical Medicine 20 (1978) 256–266.
[44] S.N. Keenan, R.C. Meex, J.C.Y. Lo, A. Ryan, S. Nie, M.K. Montgomery, M.J. Watt, Perilipin 5 deletion in hepatocytes remodels lipid metabolism and causes hepatic insulin resistance in mice, Diabetes 68 (2019) 543–555.
[45] M. Bosma, L.M. Sparks, G.J. Hooiveld, J.A. Jorgensen, S.M. Houten, P. Schrauwen, S. Kersten, M.K. Hesselink, Overexpression of PLIN5 in skeletal muscle promotes oxidative gene expression and intramyocellular lipid content without compromising insulin sensitivity, Biochim. Biophys. Acta 1831 (2013) 844–852.
[46] N.M. Pollak, D. Jaeger, S. Kolleritsch, R. Zimmermann, R. Zechner, A. Lass, G. Haemmerle, The interplay of protein kinase a and perilipin 5 regulates cardiac lipolysis, J. Biol. Chem. 290 (2015) 1295–1306.
[47] M.K. Montgomery, R. Mokhtar, J. Bayliss, H.C. Parkington, V.M. Suturin, C. R. Bruce, M.J. Watt, Perilipin 5 deletion unmasks an endoplasmic reticulum stress-fibroblast growth factor 21 Axis in skeletal muscle, Diabetes 67 (2018) 594–606.
[48] R.A. Mohktar, M.K. Montgomery, R.M. Murphy, M.J. Watt, Perilipin 5 is dispensable for normal substrate metabolism and in the adaptation of skeletal muscle to exercise training, Am. J. Physiol. Endocrinol. Metab. 311 (2016) E128–E137.
[49] J.H. Veerkamp, T.B. van Moerkerk, J.F. Glatz, J.G. Zuurveld, A.E. Jacobs, A. J. Wagenmakers, 14CO2 production is no adequate measure of [14C]fatty acid oxidation, Biochemical medicine and metabolic biology 35 (1986) 248–259.
[50] A.P. Bailey, G. Koster, C. Guillermier, E.M. Hirst, J.I. MacRae, C.P. Lechene, A. D. Postle, A.P. Gould, Antioxidant role for lipid droplets in a stem cell niche of Drosophila, Cell 163 (2015) 340–353.
[51] I. Bildirici, W.T. Schaiff, B. Chen, M. Morizane, S.Y. Oh, M. O'Brien, C. Sonnenberg-Hirche, T. Chu, Y. Barak, D.M. Nelson, Y. Sadovsky, PLIN2 is essential for trophoblastic lipid droplet accumulation and cell survival during hypoxia, Endocrinology 159 (2018) 3937–3949.
[52] P. Kumar, A. Nagarajan, P.D. Uchil, Analysis of Cell Viability by the Lactate Dehydrogenase Assay, Cold Spring Harbor Protocols, 2018, 2018.
[53] C. Depre, J.L. Vanoverschelde, H. Taegtmeyer, Glucose for the heart, Circulation 99 (1999) 578–588.
[54] S. Kolleritsch, B. Kien, G. Schoiswohl, C. Diwoky, R. Schreiber, C. Heier, L. K. Maresch, M. Schweiger, T.O. Eichmann, S. Stryeck, P. Krenn, T. Tomin, D. Kolb, T. Rulicke, G. Hoefler, H. Wolinski, T. Madl, R. Birner-Gruenberger, G. Haemmerle, Low cardiac lipolysis reduces mitochondrial fission and prevents lipotoxic heart dysfunction in Perilipin 5 mutant mice, Cardiovasc. Res. 116 (2) (2020) 339–352, https://doi.org/10.1093/cvr/cvz119.
[55] G. Haemmerle, A. Lass, R. Zimmermann, G. Gorkiewicz, C. Meyer, J. Rozman, G. Heldmaier, R. Maier, C. Theussl, S. Eder, D. Kratky, E.F. Wagner, M. Klingenspor, G. Hoefler, R. Zechner, Defective lipolysis and altered energy metabolism in mice lacking adipose triglyceride lipase, Science 312 (2006) 734–737. New York, N.Y.
[56] H. Wang, M. Bell, U. Sreenivasan, H. Hu, J. Liu, K. Dalen, C. Londos, T. Yamaguchi, M.A. Rizzo, R. Coleman, D. Gong, D. Brasaemle, C. Sztalryd, Unique regulation of adipose triglyceride lipase (ATGL) by perilipin 5, a lipid droplet-associated protein, J. Biol. Chem. 286 (2011) 15707–15715.
[57] J.G. Granneman, H.P. Moore, E.P. Mottillo, Z. Zhu, Functional interactions between Mldp (LSDP5) and Abhd5 in the control of intracellular lipid accumulation, J. Biol. Chem. 284 (2009) 3049–3057.
[58] M. Bosma, R. Minnaard, L.M. Sparks, G. Schaart, M. Losen, M.H. de Baets, H. Duimel, S. Kersten, P.E. Bickel, P. Schrauwen, M.K. Hesselink, The lipid droplet coat protein perilipin 5 also localizes to muscle mitochondria, Histochem. Cell Biol. 137 (2012) 205–216.

[59] F.K. Huynh, M.F. Green, T.R. Koves, M.D. Hirschey, Measurement of fatty acid oxidation rates in animal tissues and cell lines, Methods Enzymol. 542 (2014) 391–405.
[60] C. Sztalryd, D.L. Brasaemle, The perilipin family of lipid droplet proteins: gatekeepers of intracellular lipolysis, Biochimica et biophysica acta. Molecular and cell biology of lipids 1862 (2017) 1221–1232.
[61] P. Zheng, Z. Xie, Y. Yuan, W. Sui, C. Wang, X. Gao, Y. Zhao, F. Zhang, Y. Gu, P. Hu, J. Ye, X. Feng, L. Zhang, Plin5 alleviates myocardial ischaemia/reperfusion injury by reducing oxidative stress through inhibiting the lipolysis of lipid droplets, Sci. Rep. 7 (2017) 42574.
[62] M.K. Montgomery, W. De Nardo, M.J. Watt, Impact of lipotoxicity on tissue "cross talk" and metabolic regulation, Physiology 34 (2019) 134–149. Bethesda, Md.
[63] R.R. Mason, R. Mokhtar, M. Matzaris, A. Selathurai, G.M. Kowalski, N. Mokbel, P. J. Meikle, C.R. Bruce, M.J. Watt, PLIN5 deletion remodels intracellular lipid composition and causes insulin resistance in muscle, Molecular metabolism 3 (2014) 652–663.
[64] R.B. Wambolt, S.L. Henning, D.R. English, Y. Dyachkova, G.D. Lopaschuk, M. F. Allard, Glucose utilization and glycogen turnover are accelerated in hypertrophied rat hearts during severe low-flow ischemia, J. Mol. Cell. Cardiol. 31 (1999) 493–502.
[65] T.J. Wang, M.G. Larson, D. Levy, E.J. Benjamin, E.P. Leip, T. Omland, P.A. Wolf, R. S. Vasan, Plasma natriuretic peptide levels and the risk of cardiovascular events and death, N. Engl. J. Med. 350 (2004) 655–663.
[66] H. Yasue, M. Yoshimura, H. Sumida, K. Kikuta, K. Kugiyama, M. Jougasaki, H. Ogawa, K. Okumura, M. Mukoyama, K. Nakao, Localization and mechanism of secretion of B-type natriuretic peptide in comparison with those of A-type natriuretic peptide in normal subjects and patients with heart failure, Circulation 90 (1994) 195–203.
[67] M. Yoshimura, H. Yasue, K. Okumura, H. Ogawa, M. Jougasaki, M. Mukoyama, K. Nakao, H. Imura, Different secretion patterns of atrial natriuretic peptide and brain natriuretic peptide in patients with congestive heart failure, Circulation 87 (1993) 464–469.